University of Tehran Press

Online ISSN: 2345-475X

DESERT

Home page: https://jdesert.ut.ac.ir/

Land Use and Land Cover Change Assessment Using Support Vector Machine and Random Forest

Amin Mousavi[1*], Sayyed Mahmoud Enjavinezhad[2], Seyed Kazem Alavipanah[1], María Fernández Raga[3], Sedigheh Maleki[2], Seyed Javad Naghibi[4]

[1] Department of Remote Sensing and GIS, Faculty of Geography, University of Tehran, Tehran, 1417853933, Iran. Email: amin_mousavi@ut.ac.ir
[2] Department of Soil Sciences, School of Agriculture, Shiraz University, Shiraz, Iran.
[3] Department of Chemistry Applied Physics, Industrial Engineering School, University of León, León, Spain.
[4] Department of Soil Sciences, School of Agriculture, Shiraz University, Shiraz, Iran and Head of Research & Extension Office, Landscape & Green Spaces Organization of Shiraz Municipality, Shiraz, 45366-78, Iran.

Article Info.

Article type:
Research Article

Article history:
Received: 16 Oct. 2025
Received in revised from: 18 Dec. 2025
Accepted: 21 Dec. 2025
Published online: 27 Dec. 2025

Keywords:
Google Earth Engine,
Landsat 8 Imagery,
Land management,
Land surface temperature,
Kappa coefficient.

ABSTRACT

This study evaluates land use and land cover (LULC) changes in Fars Province, Iran, using machine learning algorithms, specifically comparing the performance of two non-parametric support vector machine (SVM) and random forest models. With rapid urbanization and agricultural expansion, accurate LULC classification is critical for environmental monitoring and land management. Applying the Google Earth Engine platform, multi-temporal Landsat 8 imagery was assessed. The findings demonstrated all classification methods presented high accuracy metrics and kappa coefficient values. The SVM algorithm attaining a mean overall accuracy of 91.42% for Landsat 8 imagery to show best performance among all evaluated methods. According to LULC change detection performed by the most accurate classification algorithm, the results indicated an increase in urban parks, gardens, and mountainous rangelands, while barren lands experienced a decline. The evaluation of LULC changes impacts on land surface temperature (LST) shows that enhanced vegetation cover played a key role in reducing LST. A remarkable decrease in both maximum and minimum LST values was observed, declining 37.31°C and 22.47°C in 2019 to 34.45°C and 19.98°C in 2023, respectively. Furthermore, the findings highlight integrating high-resolution satellite imagery with the SVM algorithm leads to achieve a highly accurate and efficient approach for LULC mapping. Consequently, this method proves to be a valuable tool for decision-making in natural resource management and urban planning in similar regions.

Cite this article: Mousavi, A., Enjavinezhad, S.M., Alavipanah, S.K., Fernández Raga, M., Maleki, S., Naghibi, S.J. (2025). Land Use and Land Cover Change Assessment Using Support Vector Machine and Random Forest. DESERT, 30 (2), DOI: 10.22059/jdesert.2025.106078

DOI: 10.22059/jdesert.2025.106078

Publisher: University of Tehran Press

1. Introduction

Changes in land use and land cover (LULC) are significant factors in environmental transformation, especially in areas undergoing swift urban growth or ecological pressure. Comprehending how landscapes change over time is crucial for assessing environmental deterioration, the pressure on water resources, and susceptibility to climate-related threats. Despite a wealth of research on LULC dynamics across different geographical areas, arid and semi-arid regions are still under-researched, even though they are highly susceptible to human impacts and climate variations (Daba & You, 2022; Silakhori *et al*., 2024). Such environments frequently experience rapid land degradation, depletion of groundwater, and loss of vegetation, rendering precise LULC monitoring essential for effective environmental management.

Recent developments in remote sensing have greatly enhanced the ability to identify and measure LULC changes through satellite images taken over various time intervals. Cloud-based platforms such as Google Earth Engine (GEE) provide effective access to extensive image archives and support large-scale spatial analysis through powerful computational resources. In these platforms, machine learning (ML) algorithms have gained significance because of their adaptability and high efficacy in complex landscape classification assignments. Algorithms like random forest (RF) and support vector machine (SVM) have shown enhanced precision in various environmental contexts and are currently extensively used for multi-temporal LULC mapping (Rahmanian *et al*., 2023; Affonso *et al*., 2023).

Monitoring LULC changes is especially crucial for assessing their effects on land surface temperature (LST). Changes in vegetation cover, soil exposure, and urban areas can directly impact thermal characteristics at the surface, resulting in localized warming or cooling effects. Many studies indicate that urban growth, decreased vegetation cover, and changes in agricultural land lead to significant rises in LST (Alavipanah *et al*., 2017; Hua & Ping, 2018). Grasping the relationship between LULC changes and LST patterns is crucial for environmental planning, particularly in watersheds experiencing climate instability, frequent droughts, or rapid land conversion.

The Shiraz watershed, situated in the Maharloo Lake basin, exemplifies a significant scenario where environmental stresses and human activities intersect. In recent decades, agricultural areas have been transformed into residential and commercial developments, speeding up landscape fragmentation. These modifications have affected local water processes, heightened surface runoff, and led to increasing surface temperatures in warm seasons. Moreover, the watershed faces risks of water shortage, salinization, and seasonal droughts, highlighting the importance of accurate evaluation of land cover alterations and their thermal effects. Although its ecological importance is recognized, there has been minimal research quantitatively assessing the merged LULC–LST interactions in this area utilizing modern ML-focused techniques.

Considering these challenges, it is evident that a systematic and precise method is required to identify LULC changes and assess their thermal effects over time. Datasets obtained from satellites, like Landsat images, provide valuable long-term records for this purpose, while incorporating ML classifiers in GEE creates an effective system for producing accurate LULC maps. Nonetheless, the effectiveness of various ML algorithms may differ based on landscape features, class spectral separability, and the quality of samples. Thus, finding the best classifier for this watershed is essential to guarantee accurate LULC mapping, which will in turn impact the dependability of LST change evaluations.

This research seeks to fill the noted gap by performing a multi-temporal examination of LULC and its connection with LST in the Shiraz watershed for the years 2019 and 2023. The key objectives of this study include: (1) Utilizing the best ML algorithm for generating accurate LULC maps; (2) Analyzing the changes in LULC through the study period; (3) Investigating the influence of LULC alterations on LST.

The findings of this study aim to aid environmental planning, risk reduction, and resource management efforts in the watershed by providing a clear insight into how land cover changes affect temperature fluctuations in a delicate ecological setting.

2. Materials and methods

2.1. Study Area

This research was carried out in the urban watershed of Shiraz, which is part of the Maharloo Lake basin, located in the central area of Shiraz city, Fars province, southern Iran. The total area of the watershed spans 41,133 ha, with geographic coordinates ranging from 632643 to 662390 in the northern latitude and from 3262310 to 3301466 in the eastern longitude, UTM zone 39 (Figure 1). According to meteorological station data, the region receives an average annual precipitation of 343.2 mm. The mean annual temperature is approximately 18°C, while the average relative humidity is recorded at 40% (IRIMO, 2019). The study area is characterized by xeric and thermic soil moisture and temperature regime, respectively (Enjavinezhad *et al*. 2025), with Aridisols and Entisols soil classifications (Keys to Soil Taxonomy, 2022). The mean elevation of the area varies around 1,484 meters above sea level. Furthermore, the land use pattern in this area is significantly influenced by climatic conditions, topographic features, and human activities.

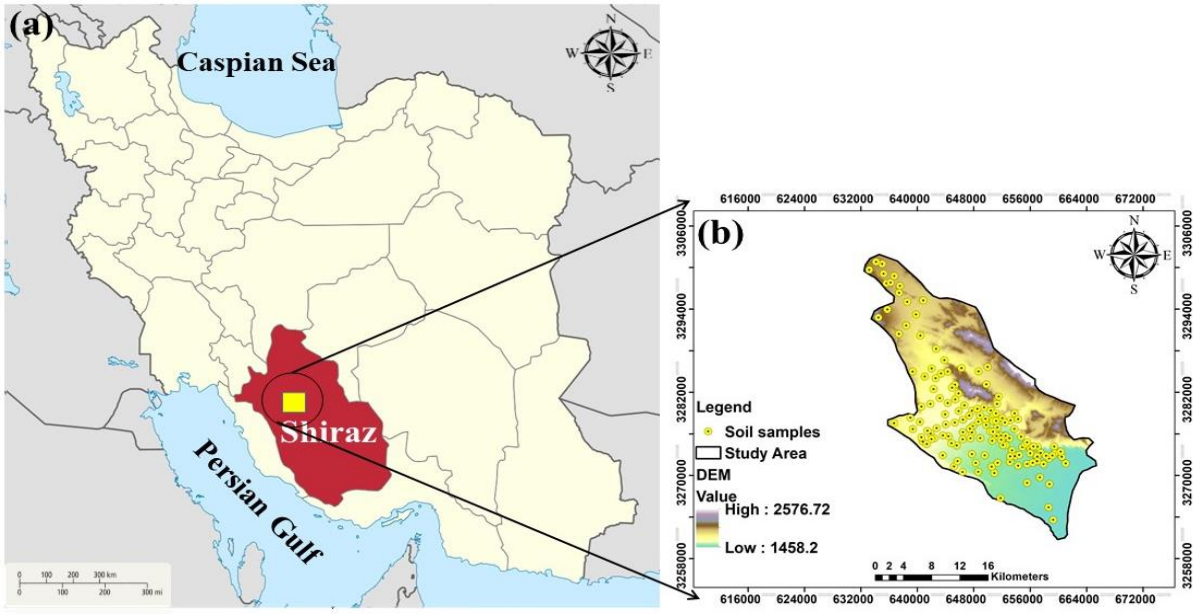

Fig. 1. Location map of Fars province in Iran (a), Location map of the study area (b)

2.2. LULC Classification Methodology

The overall workflow of this study is illustrated in Figure 2, outlining the step-by-step process undertaken in the research. Various approaches exist for detecting LULC changes using satellite imagery data (Zhu, 2017). One of the most straightforward yet effective methods involve comparing RS data collected at multiple time points (Homer *et al*., 2020). Landsat 8 satellite images from July 2019 and July 2023 were utilized to generate LULC maps in the study area. Additionally, the reference data for this research include satellite imagery, which is available for the study years through GEE.

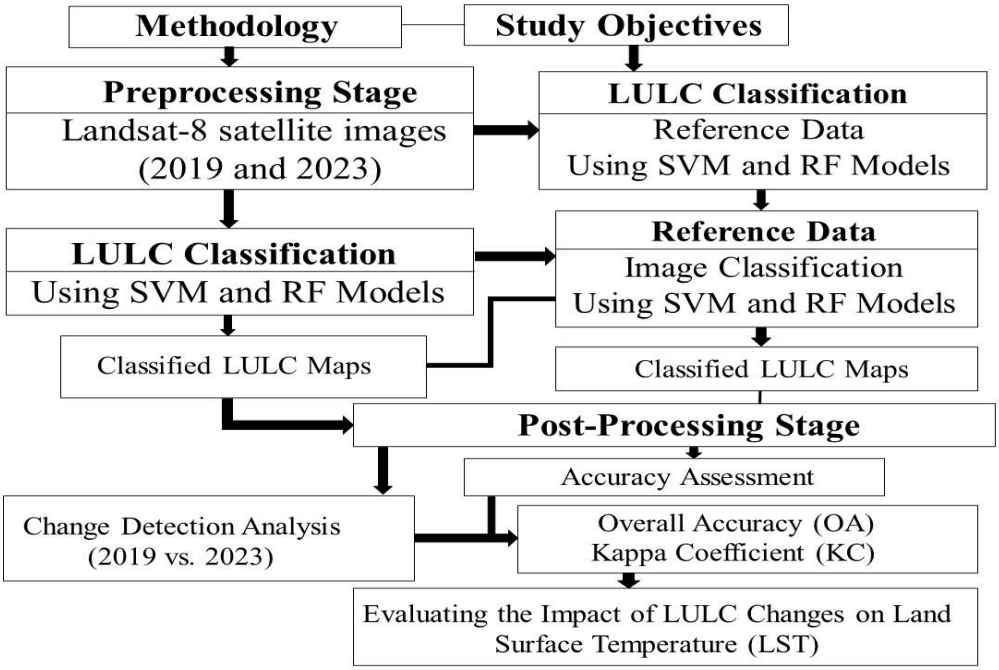

Fig. 2. Flowchart (Overview) of the research methodology

2.3. Preprocessing

The cloud-based computing platform Google Earth Engine (GEE) was utilized to create image collections and process time series. All surface reflectance products from Landsat 8 within the study area were used as the primary input for classification, allowing for the extraction of spectral-temporal metrics. After that, necessary filters and corrections, including cloud cover removal, were then applied. For cloud cover removal, the technique proposed by Simoni *et al*. (2015) was implemented within the GEE system. Pixels affected by cloud conditions or missing data were excluded from all images using a cloud mask.

Field observations revealed that the study area consists of four LULC classes: barren land, garden, urban park, and mountainous rangeland (Table 1). To improve classification accuracy, in addition to the spectral bands, several spectral indices were utilized, including the NDVI, normalized difference water index (NDWI), normalized difference built-up index (NDBI), bare soil index (BSI), and soil-adjusted vegetation index (SAVI). These spectral indices were combined with Landsat 8 data for each year to create a composite image, which was then processed using a median filter to form a single image (Loukika *et al*., 2021). Subsequently, reference data (n = 148) were randomly collected from high-resolution images in GEE and

used for LULC classification. Of the reference data, 70% (n = 104) were utilized as training samples for classifying the satellite images, while the remaining 30% (n = 44) were reserved for validating the classification results. Finally, using supervised classification techniques, the Landsat 8 images were classified to generate LULC maps for the year 2023.

Table 1. Land-use/land-cover classes, area, and balanced reference sample allocation used for supervised classification

Land Use Class	Area (ha)	Number of Samples
Barren Land	1398.31	30
Garden	426.50	30
Urban Park	56.87	30
Mountainous Rangelands	512.27	30

2.4. Supervised machine learning classification algorithms

Two widely used and popular classification algorithms, SVM and RF, were applied for supervised classification.

2.4.1. Support Vector Machine (SVM)

SVM is a supervised learning algorithm widely used for both classification and regression tasks. Its primary objective is to identify an optimal hyperplane that effectively separates data points belonging to different classes. By maximizing the margin between the data points and the decision boundary, SVM enhances classification accuracy. Due to its strong capability in handling nonlinear problems and its flexibility through the use of various kernel functions such as linear, polynomial, and radial basis function (RBF) kernels SVM has become a popular choice for complex pattern recognition and data analysis applications (Talukdar *et al*., 2020).

2.4.2. Random Forest (RF)

RF is a supervised ML technique used for classification and regression tasks. This algorithm consists of a collection of DT that are independently constructed (Breiman, 2001). Each tree is built by randomly selecting a subset of data and features. The final results are obtained by averaging or voting the outcomes from all the trees. Due to its ability to reduce variability and enhance accuracy, particularly in complex problems with high-dimensional data, this algorithm is highly effective (Maleki *et al*., 2020).

2.5. Assessment of predictive accuracy

Evaluating the accuracy of RS data is one of the most crucial and final steps in determining the informational value of the output data for the end user (Rwanga and Ndambuki, 2017). The use of various statistical methods for assessing the accuracy of LULC classification can aid in understanding the reliability of the results and determining whether the research objectives have been met (Wang *et al*., 2019). The accuracy of LULC is evaluated by comparing the classified map, produced by different classifiers, with reference data for validation (Daba & You, 2022). In this study, the accuracy of the LULC maps generated in GEE was validated using Google Earth imagery as the data source.

The change detection after classification was conducted using a comparison method based

on post-classification. LULC maps for 2019 and 2023 were independently classified and then compared pixel-by-pixel to detect transitions among land-use classes and measure their spatial and areal variations.

The effect of LULC changes on land surface temperature (LST) was assessed by obtaining LST values linked to each LULC category for the two years. Mean LST values were computed for each category and analyzed between 2019 and 2023 to evaluate how various land-use changes affected surface temperature differences.

Land surface temperature (LST) was obtained from the thermal infrared data (Band 10) of Landsat 8. Digital numbers were transformed into spectral radiance, subsequently converted to at-sensor brightness temperature, and then subjected to land surface emissivity correction through an NDVI-based emissivity methodology. This standard method guaranteed physically consistent estimation of LST.

3. Results

3.1. LULC Classification Maps

Figure 3 illustrates the LULC classification maps derived from Landsat 8 images using the SVM and RF models. As observed, the SVM classifier mistakenly classified barren land as urban parksin both 2019 and 2023. This observation is described qualitatively and does not serve as a numerical assessment of class-level precision.

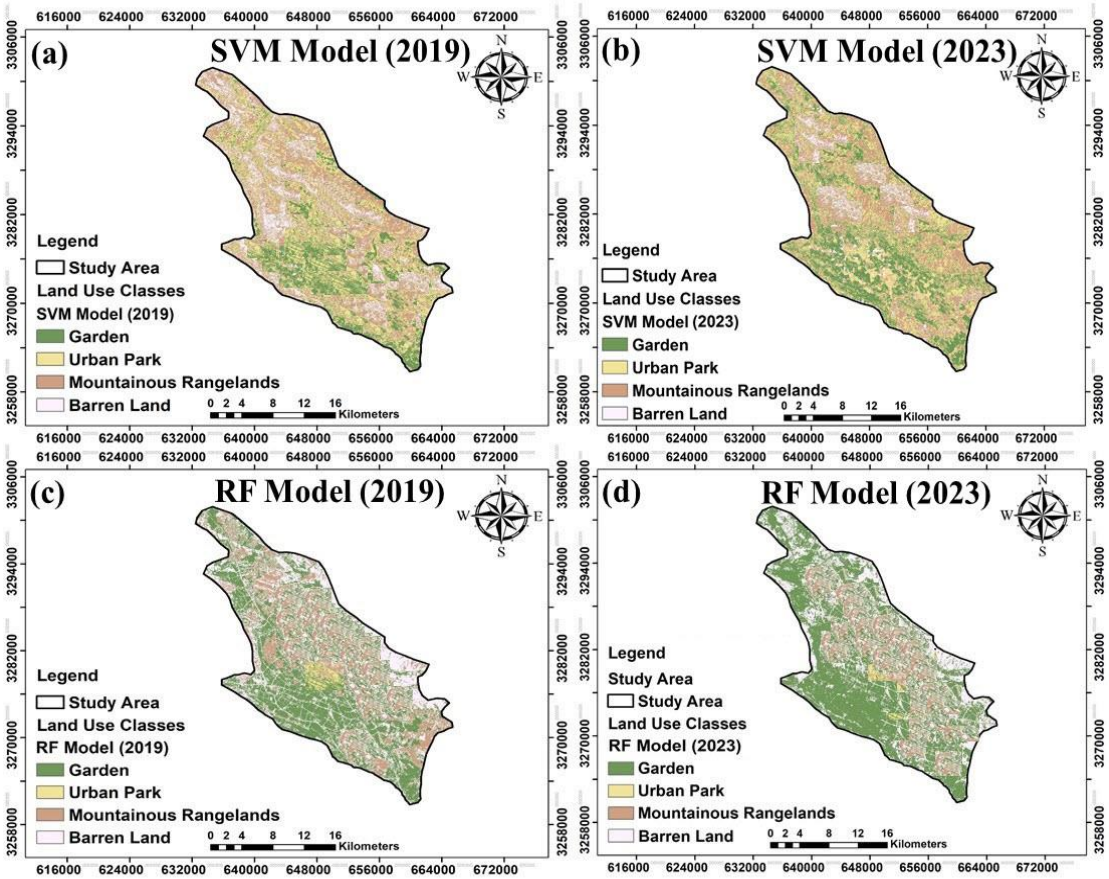

Fig. 3. LULC classification maps derived from Landsat 8 data using the SVM and RF models for the years 2019 and 2023

The RF classifier misclassified some barren lands and gardens as gardens and urban parks (Figure 3). It also incorrectly identified certain barren areas as urban zones and a few gardens as mountainous rangelands.

A comparison between the classified images and the actual land use conditions during the studied years reveals that the SVM classifier, utilizing Landsat 8 satellite imagery, achieved superior accuracy and exhibited a stronger correspondence with real-world land use patterns. Conversely, the RF classifier demonstrated a higher rate of misclassification, erroneously assigning certain pixels to incorrect land use categories.

3.2. Accuracy Evaluation

After classifying LULC using the selected classifiers, the overall accuracy and kappa coefficient were computed to validate the classified LULC maps within GEE. A comparative assessment of the SVM and RF classifiers, based on overall accuracy and kappa coefficient, is summarized in Table 2.

Table 2. Kappa coefficient and overall accuracy for SVM and RF models based on Landsat 8 data

Study Year	SVM Model		RF Model	
	Overall accuracy	Kappa coefficient	Overall accuracy	Kappa coefficient
2019	90.80	0.87	89.50	0.86
2023	92.04	0.90	91.20	0.88

Our validation results revealed that the SVM classifier exhibited the highest performance, achieving overall accuracies of 90.8% and 92.04% with kappa coefficients of 0.87 and 0.90 for the years 2019 and 2023, respectively. Similarly, the RF classifier demonstrated overall accuracies of 89.50% and 91.20%, along with kappa coefficients of 0.86 and 0.88 during the same period. These findings indicate that the SVM provides superior accuracy in generating LULC maps using Landsat satellite imagery.

3.3. Land use and land cover changes

The data reveal a 12.49% increase in garden areas, a 13.57% increase in urban parks, and a 4.37% increase in mountainous rangelands, whereas barren lands have declined by 33.84%. Analyzing satellite imagery from this period validates these findings, indicating that, over the four years, certain barren lands have been converted into gardens, industrial zones, and residential areas. Furthermore, the relative increase in annual precipitation, the decrease in temperatures, and the cessation of prolonged drought conditions in recent years have led to an increase in water resources in the mountainous rangelands, resulting in a slight expansion of their total area.

The classification results of land-use/land-cover (LULC) obtained from Landsat imagery show clear spatial variations throughout the study area from 2019 to 2023 (Figure 4). The maps show an increase in vegetated land-cover types, such as gardens, urban parks, and mountainous rangelands, along with a decrease in barren land regions. These variations are spatially diverse and differ across various regions of the watershed, indicating site-specific land-use patterns. The recorded LULC changes indicate a significant alteration in surface traits, as vegetated classes comprised a greater share of the landscape in 2023 than in 2019. The spatial rearrangement of land-cover types emphasizes alterations in land management and land-use practices in the study area throughout the examined timeframe.

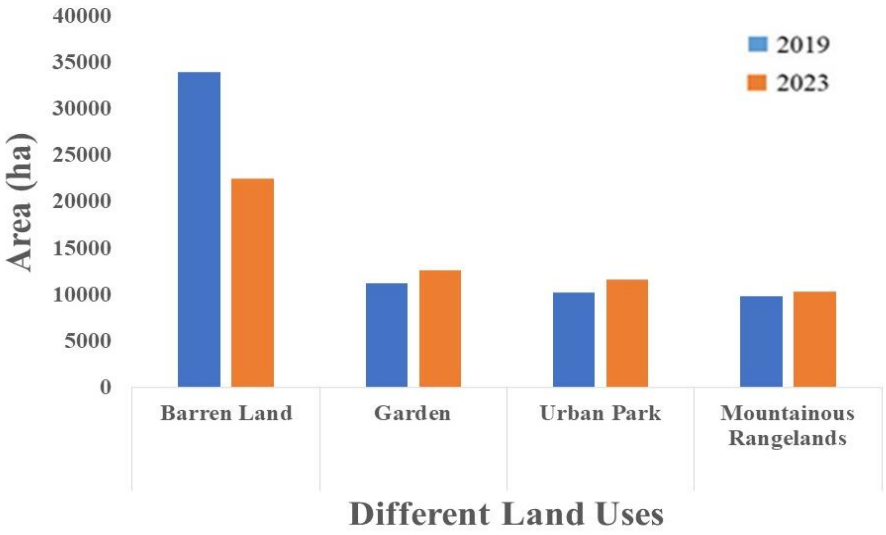

Fig 4. LULC change trend from 2019 to 2023 using the SVM classifier with Landsat 8 imagery

3.5. NDVI Spatial Patterns and Temporal Variations

The NDVI distribution maps for 2019 and 2023 (Figure 5) illustrate distinct variations in vegetation greenness across the two years. Regions defined by gardens, city parks, farmland, and hilly rangelands consistently show elevated NDVI values, while barren land regions reveal reduced values. Table 3 presents a summary of quantitative NDVI statistics. The highest NDVI value rose from 0.58 in 2019 to 0.69 in 2023, signifying improved vegetation greenness in certain regions of the study area.

The lowest NDVI value rose from -0.14 to -0.06 in that timeframe. These changes are especially noticeable in regions where the land cover shifted from bare ground to vegetated types. In general, the NDVI findings indicate a notable enhancement in vegetation health throughout the study region from 2019 to 2023, with spatial trends closely aligned to the distribution of various LULC classes.

Table 3. The variations in NDVI values over the study years

Year	NDVImin	NDVImax
2019	-0.14	0.58
2023	-0.06	0.69

As non-evaporative surfaces expand and vegetation cover declines, surface temperatures tend to increase (Shahfahad, Kumari *et al.*, 2020). To understand the influence of LULC changes on LST in our study, we created LST and NDVI distribution maps using Landsat 8 satellite imagery on the GEE. This enabled a thorough examination of their connection (Figure 5). Spatial links were noted between NDVI fluctuations and LST trends in the research region. This research interprets the connection between LST and NDVI through relative spatial patterns instead of a definitive causal or quantitative relationship. Spatial associations were observed between variations in NDVI and differences in LST across different land-use/land-cover classes. Considering the moderate spatial resolution of Landsat images and the natural uncertainty linked to land-cover classification, the observed LST–NDVI relationship ought to

be viewed as a comparative and descriptive examination of surface thermal patterns, instead of a conclusive interpretation of the factors influencing temperature.

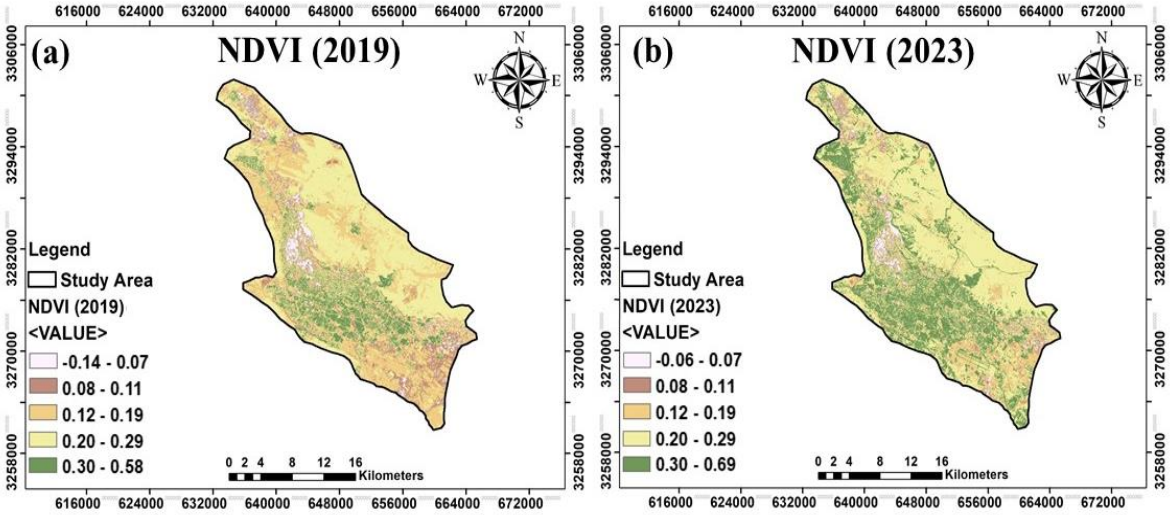

Fig. 5. NDVI distribution maps for 2019 and 2023

3.6. Land Surface Temperature (LST) Distribution and Changes

Figure 6 displays the spatial distribution of land surface temperature (LST) for the years 2019 and 2023. Areas with barren land and constructed surfaces mainly exhibit higher LST values, whereas vegetated regions and water bodies are linked to lower temperatures.

Geographically, the northern, southern, and eastern sections of the study region display comparatively elevated LST values, while the central zones, defined by farmland, gardens, and hilly rangelands, reveal lower surface temperatures. This spatial difference remains consistent throughout both study years.

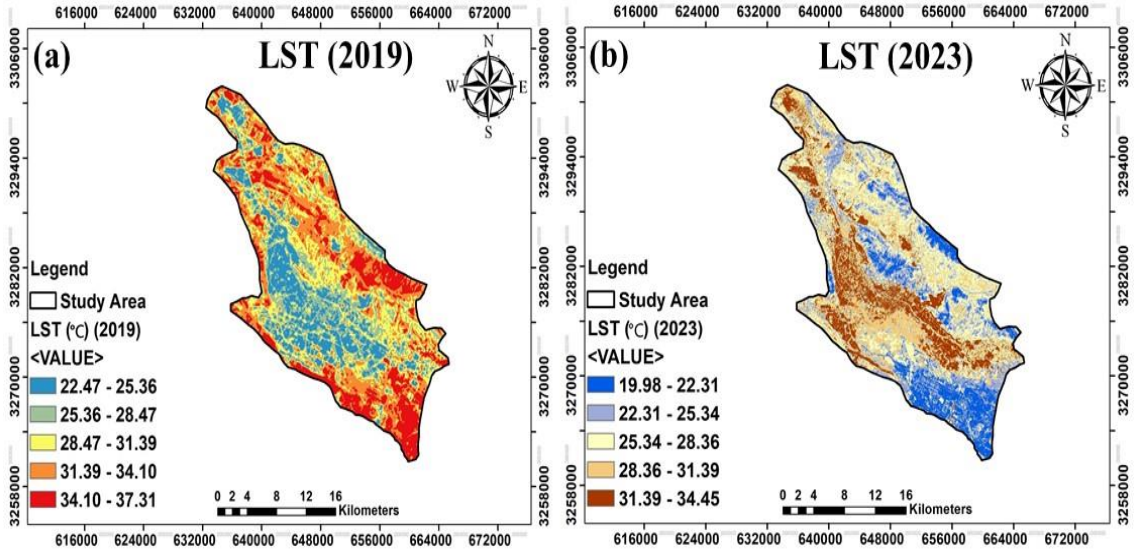

Fig. 6. LST map for the years 2019 and 2023

The quantitative LST statistics shown in Table 4 reveal a decline in both maximum and minimum LST values throughout the study period. The highest LST fell from 37.31 °C in 2019 to 34.45 °C in 2023, and the lowest LST dropped from 22.47 °C to 19.98 °C. These findings indicate significant alterations in surface thermal conditions linked to LULC changes over the study period. These results suggest that multiple factors, including the type of vegetation, plant density, and human activities, can influence LST. Modifications in land cover and other surface characteristics, such as land use changes, vegetation growth, and urbanization, can lead to notable shifts in surface temperatures. When analyzing land cover changes and their effects on surface energy, special attention must be paid to these influencing factors.

The results of recent research conducted by Damayanti *et al*. (2023) showed an increase in vegetation cover leads to a decrease in LST, whereas the drying of lakes results in its increase. Similarly, they concluded that changes in soil surface temperature are closely related to land cover modifications, with a noticeable rise in soil temperatures in areas where land use changes occurred. In general, it can be concluded that land use changes from barren land to agricultural areas, gardens, urban parks and mountainous rangelands positively influence the spatial distribution of LST. The expansion of vegetative cover and enhanced evapotranspiration in these areas contribute to lower LST, thereby potentially improving environmental conditions and mitigating the impacts of climate change. Continuous and detailed monitoring of such changes using RS data can provide critical insights for effective natural resource management and environmental planning.

Table 4. LST change values over the study year

Year	LSTmin (ºC)	LSTmax (ºC)
2019	22.47	37.31
2023	19.98	34.45

As observed, barren lands and urban parks exhibit the highest LST values (Figure 6), whereas water bodies and vegetated regions demonstrate lower temperatures. The spatial analysis of LST over the study period indicates that changes in LULC have directly influenced surface temperature. Specifically, areas where barren lands have been converted into gardens, urban parks, and mountainous rangelands (increasing NDVI) have experienced a reduction in LST. Furthermore, the maps reveal that the northern, southern and eastern parts of the study area, predominantly consisting of barren lands and urban zones, exhibits the highest LST values. In contrast, the central region, characterized by agricultural fields, expanded gardens, and mountainous rangelands, demonstrates lower surface temperatures. Research was done by Liping *et al*. (2018) showed the conversion of barren lands into agricultural areas typically results in a reduction of LST, as newly established vegetation can absorb a substantial amount of solar radiation and enhance the evapotranspiration process, which in turn contributes to temperature reduction. This effect is particularly pronounced in regions where irrigation systems are utilized. For example, a study conducted in China revealed that the transition from barren land to agricultural use led to a decrease in the average LST by up to 2°C in the studied area (Zhu *et al*., 2017).

Gardens are typically established in semi-arid and barren regions due to their low water requirements and adaptability to dry conditions. These green spaces, including parks, gardens,

gardens, and other vegetated areas, can play a significant role in reducing LST, particularly during the warmer months. For instance, a study conducted in the Mediterranean region revealed that olive gardens reduced LST by an average of 3°C compared to the surrounding barren lands (Alganci *et al*., 2018).

4. Discussion

The results indicated that SVM offers a superior representation of spectrally intricate urban and constructed regions. This is due to SVM's capability to handle high-dimensional input spaces featuring non-linear class boundaries (Foody & Mathur, 2004). In contrast, the RF model better characterizes continuous vegetation covers like croplands and forests. This advantage stems from the ensemble characteristics of the RF algorithm, providing enhanced resilience against noise and fluctuations in data (Maleki *et al*., 2020; Mousavi *et al*., 2023). Visual evaluation of the classification maps showed that SVM generated outputs that were more spatially cohesive with reduced random classification noise, especially in fragmented landscapes and transitional zones. The ongoing study emphasizes the importance of implementing a multi-faceted assessment framework that simultaneously integrates statistical, spatial, and semantic precision. This method offers a better understanding of how and why SVM classifiers can statistically excel over other techniques in specific situations, particularly in dynamic or spectrally diverse settings. The noted disparities in pixel classifications in the LULC maps can be attributed to differences in spectral responses, variations in model parameter tuning, and discrepancies in algorithm effectiveness. Past research has emphasized that LULC classification via satellite imagery is affected by various factors, such as the satellite type, weather conditions, classification methods, and unique features of the study location. Thus, alterations in the study area, dataset volume, and atmospheric, lighting, or geometric factors may influence the classification results and precision (McCarty *et al*., 2020; Nasiri *et al*., 2022; Yuh *et al*., 2023). Incorporating these contextual elements in the Discussion enhances the comprehension of the noted differences and underlines the interpretation of the classification findings showcased in this research.

Bouslihim *et al*. (2022) examine into the effectiveness of two ML algorithms, RF and SVM, for LULC classification using Landsat 9 and Sentinel-2 imagery. Their findings indicated that combining Sentinel-2 data with the SVM classifier yielded the most precise classification. Similarly, Abdi (2020) explored the accuracy of non-parametric classification algorithms in south-central Sweden. A comparison of four algorithms SVM, RF, extreme gradient boosting (XGBoost), and deep learning (DL) showed that the SVM classifier achieved the highest overall accuracy.

Using the classified results, changes over time in vegetation cover were examined. The findings show that the overall vegetative cover in the research region rose from 31267.42 ha in 2019 to 34483.64 ha in 2023 (Figure 4). These modifications are also apparent in the NDVI distribution map (Figure 5). The results indicate a notable correlation among land-use/land-cover (LULC) alterations, vegetation changes, and trends in land surface temperature (LST) within the research region. In particular, the increase in green land-cover types like gardens, city parks, and hilly rangelands correlates with elevated NDVI values and reduced surface temperatures.

The noted rise in NDVI signifies enhancements in plant density and surface greenness, especially in regions where unproductive land has been transformed into cultivated or semi-natural vegetation. This pattern aligns with earlier research carried out in semi-arid and

Mediterranean settings, where vegetated regions typically show greater NDVI values than bare ground because of denser canopy cover and better moisture availability (Alganci *et al*., 2018). The alignment between the current results and prior studies strengthens the dependability of the noted vegetation trends. The spatial arrangement of LST highlights the cooling effect of vegetation cover. Results indicate that barren zones with minimal vegetation show elevated LST values, whereas areas with vegetation and irrigation reveal reduced surface temperatures. This disparity can be attributed to variations in surface energy balance, as vegetation lowers surface heating via shading and evapotranspiration mechanisms. Similar associations between LULC and LST have been frequently documented, especially in research focusing on changes in land cover from barren or empty zones to agricultural or verdant areas (Zhu *et al*., 2017; Liping *et al*., 2018). The noted reduction in both maximum and minimum LST values during the study period indicates that recent land-cover alterations have played a role in regulating surface thermal conditions. This effect is particularly significant in semi-arid urban watersheds, where surface warming is frequently exacerbated by large barren zones and developed regions. Earlier research has indicated that the growth and increase of gardens and urban green areas can greatly lower surface temperatures, especially in warm seasons (Alganci *et al*., 2018), which aligns closely with the spatial patterns found in this research. The results indicate that changes in LULC from uninhabited or barren regions to vegetated land types positively influence vegetation indices and surface temperature patterns. The alignment of this study's findings with earlier research underscores the significance of vegetation-focused land management approaches for enhancing environmental quality and reducing surface heat. Ongoing observation of LULC, NDVI, and LST through remote sensing data offers essential insights for sustainable land-use planning and climate adaptation approaches in semi-arid areas.

5. Conclusion

In this study, the ability of various classifiers on the GEE platform to produce accurate LULC maps was evaluated with the aim of identifying the best-performing classifier. The results indicated that the SVM classifier, when applied to Landsat 8 imagery in the study area, which includes various land use types such as barren lands, gardens, urban parks, and mountainous rangelands, outperformed other classifiers. The analysis of land cover changes during the study period revealed that the total vegetative cover increased from 31267.42 ha in 2019 to 34483.64 ha in 2023. This increase in vegetative cover led to a rise in NDVI and a decrease in LST. Additionally, cloud-based platforms such as GEE and Landsat 8 satellite data have significantly contributed to the enhancement of LULC mapping and monitoring. Overall, the accuracy assessment revealed minor variations in overall accuracy and kappa coefficient values among the different classifiers. Given that an overall accuracy above 70% is deemed acceptable, and a kappa coefficient between 0.40 and 0.85 signifies good agreement (with 0.86 - 1 indicating excellent agreement, according to Congalton, 1991), both the SVM and RF models proved effectiveness and practicality for generating LULC maps from Landsat 8 data. However, the SVM algorithm truly emerged as the most suitable classifier for LULC mapping in this context. Consequently, LULC classification using high-resolution spatial imagery and the SVM algorithm on the GEE platform proves to be an accurate and efficient method for assessing land use and cover changes over different periods. Therefore, this approach can serve as a valuable tool in natural resource and urban planning, including land use planning and water and soil management. However, it is important to consider that while satellite data

offers numerous advantages in environmental studies, some limitations exist. As, this method encounters challenges in areas affected by clouds and fog, necessitating the use of radar data. Future research should explore the use of other classification algorithms, such as deep learning techniques, to improve classification accuracy and investigate the integration of satellite data with additional datasets, such as RS, field data, and modeling outputs, to enhance the quality and precision of land use and cover maps.

Author Contributions

All authors contributed to the conception and design of the study. SME, and SJN prepared the samples and performed the experiments. AM, SME and MFR analyzed the data and conducted the modelling procedures. AM wrote the first draft of the manuscript with support from SKA and SME. SKA and SME provided critical feedback and contributed to the interpretation of the results. All authors substantially contributed to the editing, reviewing, and final approval of the manuscript.

Data Availability Statement

Data available on request from the authors.

Acknowledgements

We are grateful to the Iran National Science Foundation (INSF) for supporting the joint postdoctoral project with the University of Tehran. We sincerely thank Professor Seyed Kazem Alavipanah for his invaluable guidance throughout this study. This research will also lay the groundwork for future collaborative efforts between the institutions.

Ethical considerations

The authors declare that no data fabrication or falsification was involved in this study.

Conflict of interest

The authors declare no conflict of interest.

References

Abdi, A. M. (2020). Land cover and land use classification performance of machine learning algorithms in a boreal landscape using Sentinel-2 data. *GIScience & Remote Sensing*, *57*(1), 1-20. https://doi.org/10.1080/15481603.2019.1650447

Affonso, A. A., Mandai, S. S., Portella, T. P., Quintanilha, J. A., Conti, L. A., & Grohmann, C. H. (2023). A comparison between supervised classification methods: study case on land cover change detection caused by a hydroelectric complex installation in the Brazilian amazon. *Sustainability*, *15*(2), 1309. https://doi.org/10.3390/su15021309

Alavipanah, S. K., Weng, Q., Gholamnia, M., & Khandan, R. (2017). An analysis of the discrepancies between MODIS and INSAT-3D LSTs in high temperatures. *Remote Sensing*, *9*(4), 347. https://doi.org/10.3390/rs9040347

Alganci, U., Sertel, E., & Kaya, S. (2018). Determination of the olive trees with object based classification of Pleiades satellite image. *International Journal of Environment and Geoinformatics*, *5*(2), 132-139. https://doi.org/10.30897/ijegeo.396713

Basheer, S., Wang, X., Farooque, A. A., Nawaz, R. A., Liu, K., Adekanmbi, T., & Liu, S. (2022). Comparison of land use land cover classifiers using different satellite imagery and machine learning techniques. *Remote Sensing*, *14*(19), 4978. https://doi.org/10.3390/rs14194978

Bouslihim, Y., Kharrou, M. H., Miftah, A., Attou, T., Bouchaou, L., & Chehbouni, A. (2022). Comparing pan-sharpened Landsat-9 and Sentinel-2 for land-use classification using machine learning classifiers. *Journal of Geovisualization and Spatial Analysis*, *6*(2), 35. https://doi.org/10.1007/s41651-022-00130-0

Breiman, L. (2001). Random forests. *Machine learning*, *45*, 5-32. https://doi.org/10.1023/A:1010933404324

Congalton, R. G. (1991). A review of assessing the accuracy of classifications of remotely sensed data. *Remote sensing of environment*, *37*(1), 35-46. https://doi.org/10.1016/0034-4257(91)90048-B

Daba, M. H., & You, S. (2022). Quantitatively assessing the future land-use/land-cover changes and their driving factors in the upper stream of the Awash River based on the CA–markov model and their implications for water resources management. *Sustainability*, *14*(3), 1538. https://doi.org/10.3390/su14031538

Damayanti, A., Khairunisa, F. I., & Maulidina, K. (2023). Impacts of Land Cover Changes on Land Surface Temperature using Landsat Imagery with the Supervised Classification Method. *Aceh International Journal of Science and Technology*, *12*(1), 116-125. https://doi.org/ 10.13170/aijst.12.1.30834

Edwards, S., Egziabher, T. B. G., & Araya, H. (2010). Successes and challenges in ecological agriculture experiences from Tigray, Ethiopia. *Tigray Project.*

Enjavinezhad, S. M., Naghibi, S. J., Shirazi, M. P., Baghernejad, M., Fernández-Raga, M., & Rodrigo-Comino, J. (2025). From fields to cities: Innovating assessment of soil quality in Southern Iran's Urban areas. *PLoS one*, *20*(5), e0321312. https://doi.org/10.1371/journal.pone.0321312

Foody, G. M., & Mathur, A. (2004). A relative evaluation of multiclass image classification by support vector machines. *IEEE Transactions on geoscience and remote sensing*, *42*(6), 1335-1343. https://doi.org/10.1109/TGRS.2004.827257

Homer, C., Dewitz, J., Jin, S., Xian, G., Costello, C., Danielson, P., ... & Riitters, K. (2020). Conterminous United States land cover change patterns 2001–2016 from the 2016 national land cover database. *ISPRS Journal of Photogrammetry and Remote Sensing*, *162*, 184-199. https://doi.org/10.1016/j.isprsjprs.2020.02.019

Hua, A. K., & Ping, O. W. (2018). The influence of land-use/land-cover changes on land surface temperature: a case study of Kuala Lumpur metropolitan city. *European Journal of Remote Sensing*, *51*(1), 1049-1069. https://doi.org/10.1080/22797254.2018.1542976

Islamic Republic of Iran Meteorological Organization (IRIMO) (2019). Tehran, Iran

Liping, C., Yujun, S., & Saeed, S. (2018). Monitoring and predicting land use and land cover changes using remote sensing and GIS techniques—A case study of a hilly area, Jiangle, China. *PloS one*, *13*(7), e0200493. https://doi.org/10.1371/journal.pone.0200493

Loukika, K. N., Keesara, V. R., & Sridhar, V. (2021). Analysis of land use and land cover using machine learning algorithms on google earth engine for Munneru River Basin, India. *Sustainability*, *13*(24), 13758. https://doi.org/10.3390/su132413758

Maleki S, Khormali F, Mohammadi J, Bogaert P, Bodaghabadi MB (2020) Effect of the accuracy of topographic data on improv ing digital soil mapping predictions with limited soil data: An application to the Iranian loess plateau. *Catena*, 195, 104810. https://doi. org/10.1016/j. catena. 2020.104810

McCarty, D. A., Kim, H. W., & Lee, H. K. (2020). Evaluation of light gradient boosted machine learning technique in large scale land use and land cover classification. *Environments*, *7*(10), 84. https://doi.org/10.3390/environments7100084

Mousavi., A., Karimi, A.R., Maleki, S., Safari, T., & Taghizadeh-Mehrjardi, R. (2023). Digital mapping of selected soil properties using machine learning and geostatistical techniques in Mashhad plain, northeastern Iran. *Environmental Earth Sciences*, *82*, 234. https://doi.org/10.1007/s12665-023-10919-x

Nasiri, V., Deljouei, A., Moradi, F., Sadeghi, S. M. M., & Borz, S. A. (2022). Land use and land cover mapping using Sentinel-2, Landsat-8 Satellite Images, and Google Earth Engine: A comparison of two composition methods. *Remote Sensing*, *14*(9), 1977. https://doi.org/10.3390/rs14091977

Rahman, A., Abdullah, H. M., Tanzir, M. T., Hossain, M. J., Khan, B. M., Miah, M. G., & Islam, I. (2020). Performance of different machine learning algorithms on satellite image classification in rural and urban setup. *Remote Sensing Applications: Society and Environment*, *20*, 100410. https://doi.org/ 10.1016/j.rsase.2020.100410

Rahmanian, S., Nasiri, V., Amindin, A., Karami, S., Maleki, S., Pouyan, S., Borz, S.A. (2023). Prediction of plant diver sity using multi-seasonal remotely sensed and Geodiversity data in a mountainous area. *Remote Sensing*, *15*(2), 387. https://doi.org/10.3390/rs15020387

Rwanga, S. S., & Ndambuki, J. M. (2017). Accuracy assessment of land use/land cover classification using remote sensing and GIS. *International Journal of Geosciences*, *8*, 611-622. https://doi.org/10.4236/ijg.2017.84033

Shahfahad, Kumari, B., Tayyab, M., Ahmed, I. A., Baig, M. R. I., Khan, M. F., & Rahman, A. (2020). Longitudinal study of land surface temperature (LST) using mono-and split-window algorithms and its relationship with NDVI and NDBI over selected metro cities of India. *Arabian Journal of Geosciences*, *13*(19), 1040. https://doi.org/10.1007/s12517-020-06068-1

Simonetti, D., Simonetti, E., Szantoi, Z., Lupi, A., & Eva, H. D. (2015). First results from the phenology-based synthesis classifier using Landsat 8 imagery. *IEEE Geoscience and remote sensing letters*, *12*(7), 1496-1500. https://doi.org/10.1109/LGRS.2015.2409982

Silakhori, E., Maleki, S., & Pourghasemi, H.R. (2024). Spatiotemporal variations in land use of Mahvelat plain in Iran using Google Earth Engine from 2011 to 2030. Chapter book In *Advanced Tools for Studying Soil Erosion Processes*. *Elsevier Inc*, 413-433. https://doi.org/10.1016/B978-0-443-22262-7.00032

Sun, L., Gao, F., Xie, D., Anderson, M., Chen, R., Yang, Y., ... & Chen, Z. (2021). Reconstructing daily 30 m NDVI over complex agricultural landscapes using a crop reference curve approach. *Remote Sensing of Environment*, *253*, 112156. https://doi.org/10.1016/j.rse.2020.112156

Szostak, M., Likus-Cieślik, J., & Pietrzykowski, M. (2021). PlanetScope imageries and LiDAR point clouds processing for automation land cover mapping and vegetation assessment of a reclaimed sulfur mine. *Remote Sensing*, *13*(14), 2717. https://doi.org/10.3390/rs13142717

Talukdar, S., Singha, P., Mahato, S., Pal, S., Liou, Y. A., & Rahman, A. (2020). Land-use land-cover classification by machine learning classifiers for satellite observations—A review. *Remote Sensing*, *12*(7), 1135. https://doi.org/10.3390/rs12071135

Wang, Y., Ziv, G., Adami, M., Mitchard, E., Batterman, S. A., Buermann, W., … & Galbraith, D. (2019). Mapping tropical disturbed forests using multi-decadal 30 m optical satellite imagery. *Remote Sensing of Environment*, *221*, 474-488. https://doi.org/10.1016/j.rse.2018.11.028

Yuh, Y.G., Tracz, W., Matthews, H.D., & Turner, S.E. (2023). Application of machine learning approaches for land cover monitoring in northern Cameroon. *Ecological Informatics*, *74*, 101955. https://doi.org/10.1016/j.ecoinf.2022.101955

Zhu, Z. (2017). Change detection using Landsat time series: A review of frequencies, preprocessing, algorithms, and applications. *ISPRS Journal of Photogrammetry and Remote Sensing*, *130*, 370-384. https://doi.org/10.1016/j.isprsjprs.2017.06.013